Dynamic Molecular Triplet Excitons Tune Lanthanide Emission Lifetime

Takuma Nakai,[a] Kaori Shima,[a] Mengfei Wang,[b,c] Sunao Shoji,[d] Takayuki Nakanishi,[e] Koji Fushimi,[b] Yasuchika Hasegawa,[b,c] and Yuichi Kitagawa*[b,c]

[a] T. Nakai, K. Shima
Graduate School of Chemical Sciences and Engineering, Hokkaido University
Kita 13, Nishi 8, Kita-ku, Sapporo, Hokkaido 060-8628 (Japan).
[b] Dr. M. Wang, Dr. K. Fushimi, Dr. Y. Hasegawa, Dr. Y. Kitagawa
Faculty of Engineering, Hokkaido University
Kita 13, Nishi 8, Kita-ku, Sapporo, Hokkaido 060-8628 (Japan).
E-mail: y-kitagawa@eng.hokudai.ac.jp
[c] Dr. M. Wang, Dr. Y. Hasegawa, Dr. Y. Kitagawa
Institute for Chemical Reaction Design and Discovery (WPI-ICReDD), Hokkaido University
Kita 21, Nishi 10, Kita-ku, Sapporo, Hokkaido 001-0021 (Japan).
[d] Dr. S. Shoji
Faculty of Engineering, Nara Women's University
Kitauoya-Nishimachi, Nara 630-8506 (Japan).
[e] Dr. T. Nakanishi
National Institute for Material Science
Namiki, Tsukuba, Ibaraki 305-0044 (Japan).

Supporting information for this article is given via a link at the end of the document.

Abstract: Optical codes generated from the emission lifetimes of lanthanide complexes have received considerable attention for their potential application in multiplexed bioimaging and anti-counterfeiting. However, such tunable lifetimes are limited to short ranges (0.01–1 ms). Herein, we describe a method that extends the emission lifetime using dynamic molecular triplet excitons in aggregation systems composed of lanthanide complexes. To demonstrate the conceptual method, molecular crystals comprising lutetium (Lu^{3+}) and luminescent lanthanide (europium: Eu^{3+} or terbium: Tb^{3+}) complexes with two organic ligands (2,2,6,6-tetramethyl-3,5-heptanedionate and 2,7-bis(diphenylphosphoryl)-phenanthrene) were prepared. These molecular crystals exhibited persistent emission *via* slow triplet exciton migration between the phenanthrene units. The extended degree of the lifetime could be controlled between 1 and 152 ms by ligand modifications. This proposed lifetime-tuning method should significantly expand the encoding capacity of lanthanide complexes.

Optical encoding is a technique to generate multiple codes by combining optical parameters such as ratiometric emission intensity and emission lifetime of luminophores.[1-4] This technique plays a crucial role in multiplexed bioimaging[5-8] and anti-counterfeiting applications.[9-12] Among the luminophores for optical encoding, trivalent lanthanide complexes are promising candidates for optical encoding owing to their distinguishable sharp emission bands (Full Width at Half Maximum (FWHM) ≈ 10 nm) originating from 4f-4f transitions.[13-21] These complexes also exhibit bright emission originating from the high absorption abilities of their organic ligands *via* energy transfer from the molecular triplet exciton.[22-24]

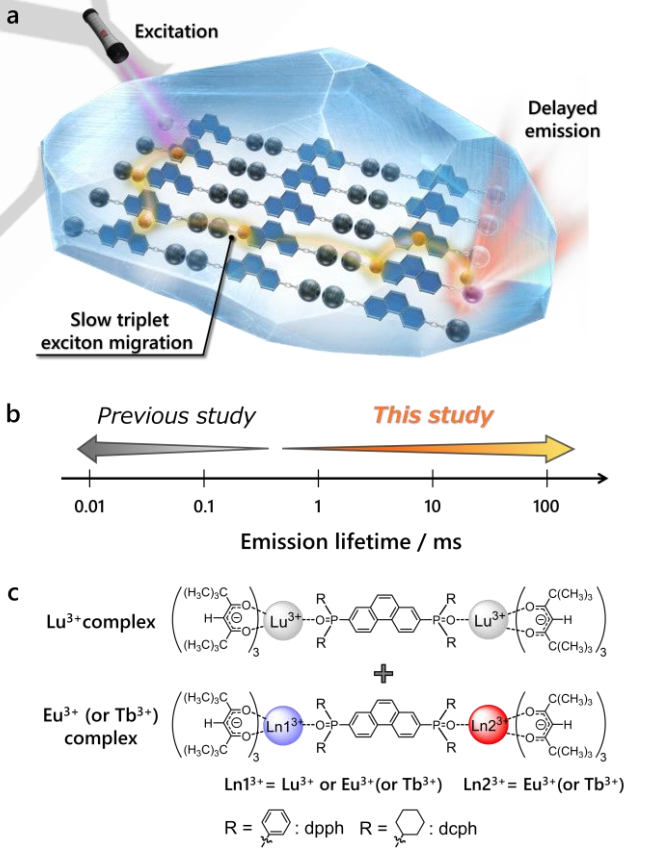

Figure 1. a: Conceptual design of this study. Black and red balls represent Lu^{3+} and Eu^{3+} (or Tb^{3+}), respectively. **b**: Emission lifetime tuning range of the lanthanide complexes in a previous study (0.01–1 ms) and this study (1–152 ms). **c**: Chemical structures of Eu^{3+}-(or Tb^{3+}-)-incorporated Lu^{3+} molecular crystals for proof-of-concept.

Recently, emission lifetime has become an emerging parameter for the effective optical encoding of lanthanide complexes because it offers detection capabilities independent of ambient background.[13-15,19] Gallis et al. achieved data storage and document security using lanthanide metal-organic frameworks (MOFs) with tunable Eu^{3+} emission lifetime by controlling the energy transfer from Eu^{3+} to Yb^{3+}.[13] Lu et al. demonstrated multiplexed bioimaging by tuning the Eu^{3+} emission lifetime based on the energy transfer from Eu^{3+} to an organic ligand.[15] However, these lifetime-tuning methods are derived from a quenching system for lanthanide emissions, and the tuning range is narrow (0.01–1 ms, **Figure 1b**). The development of a new method for extending the lifetime of lanthanide complexes will significantly expand their encoding capacities.

Herein, we describe a new method for emission lifetime tuning utilizing the slow triplet exciton migration between the organic ligands in aggregated lanthanide complexes (**Figure 1a**). This slow exciton migration results in delayed formation of lanthanide-emitting states, leading to an extended emission lifetime. To demonstrate the proof-of-concept, luminescent Eu^{3+}- (or Tb^{3+}-)-incorporated Lu^{3+} molecular crystals comprising one neutral phenanthrene-based ligand (dpph: 2,7-bis(diphenylphosphoryl)phenanthrene), **Figure 1c**) and six anionic β-diketonate ligands (tmh: 2,2,6,6-tetramethyl-3,5-heptanedionate) were designed. The dpph ligand, encapsulated by the bulky anionic tmh ligands, exhibited a long-lived triplet state (τ = 47 ms[25]), which was selected to facilitate an efficient high triplet-triplet energy transfer (TTET) between the dpph ligands. Non-luminescent Lu^{3+} (lowest excited state: ~80,000 cm^{-1} [26]) also promotes TTET in the crystals [27], resulting in delayed emission of Eu^{3+} (or Tb^{3+}) (see **Supplementary Note 1** for a discussion of systems with other non-luminescent lanthanide ions). The delayed emission lifetime can be tuned by controlling the Eu^{3+} (or Tb^{3+}) molar ratio. Another type of phenanthrene-based ligand (dcph: 2,7-bis(dicyclohexylphosphoryl)phenanthrene) was prepared to demonstrate tunable optical codes *via* ligand modification. The present dynamic triplet exciton system significantly expands optical encoding capacities to develop multiplexed bioimaging and anti-counterfeiting applications.

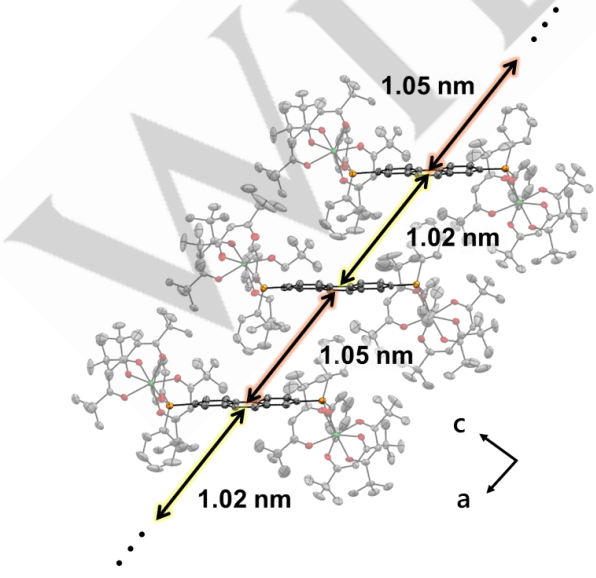

Figure 2. X-ray crystal structure of **Lu_2-dpph** viewed along b-axis (50% probability ellipsoids). The distances were calculated based on the centroids of phenanthrene units.

The $[Lu_2(tmh)_6dpph]$ (where **Lu_2-dpph**) was prepared using a previously reported method.[25] Single-crystal X-ray diffraction (XRD) analysis showed seven-coordinated dinuclear structures, consisting of two $Lu(tmh)_3$ units connected by a dpph ligand (Crystallographic data are listed in **Table S1**, Supporting Information). In the X-ray crystal structure, each **Lu_2-dpph** unit is surrounded by two adjacent **Lu_2-dpph** units (**Figure 2** and **S14**). The distances between the phenanthrene units were determined to be 1.02 and 1.05 nm.

The preparation and identification of $[Eu_2(tmh)_6dpph]$ (**Eu_2-dpph**) and $[Tb_2(tmh)_6dpph]$ [25] (**Tb_2-dpph**) were similar to those of **Lu_2-dpph** (**Figure S15**, crystallographic data are shown in **Table S1**). The photophysical measurements were performed in the crystalline state. The emission spectrum (**Figure 3a**) of **Eu_2-dpph** exhibits emission bands at approximately 578, 587, 611, 648, and 701 nm, which are assigned to the $^5D_0 \rightarrow {}^7F_J$ (J = 0, 1, 2, 3, and 4, respectively) transitions of Eu^{3+}. For **Tb_2-dpph**, emission bands at approximately 490, 548, 582, 616, and 659 nm were observed. These emission bands are attributed to the $^5D_4 \rightarrow {}^7F_J$ (J = 6, 5, 4, 3, and 2, respectively) transitions of Tb^{3+}.[25] The excitation spectra showed characteristic vibronic signals at approximately 346 and 362 nm in the UV region (**Figure S16**), indicating the effective emission *via* energy transfer from the dpph ligands. The emission decay curves of **Eu_2-dpph** and **Tb_2-dpph** (**Figure 3b**) were fitted to single-exponential function. Emission lifetimes for **Eu_2-dpph** and **Tb_2-dpph** were independent of the excitation wavelength (dpph excitation: τ_{Eu} = 0.55 ms, τ_{Tb} = 0.83 ms (λ_{ex} = 356 nm) and lanthanide excitation: τ_{Eu} = 0.55 ms (λ_{ex} = 510 nm, **Figure S18**), τ_{Tb} = 0.87 ms (λ_{ex} = 495 nm)). These results indicate the absence of delayed emission *via* intermolecular triplet exciton migration (**Figure 3c** and **Figure S19**, details of the excited state dynamics are given in **Supplementary Note 2**), which is caused by a very fast energy transfer from the organic ligands to the lanthanide ions.[28-30]

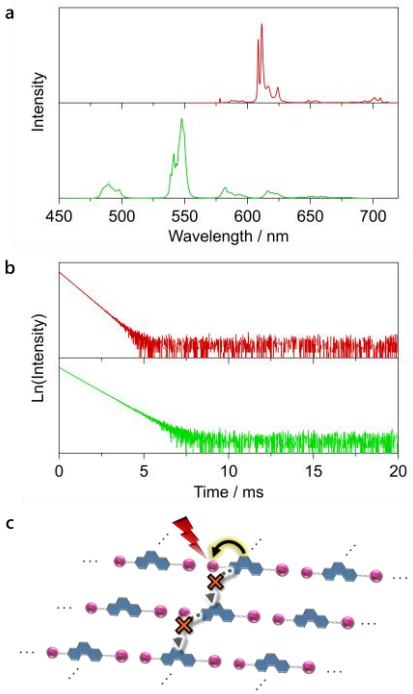

Figure 3. a: Emission spectra (λ_{ex} = 356 nm, crystalline state, 293 K) of **Eu_2-dpph** (upper) and **Tb_2-dpph** (lower) under degassed condition. **b**: Emission decay curves (λ_{ex} = 356 nm, crystalline state, 293 K) of **Eu_2-dpph** (upper, λ_{em} = 611 nm) and **Tb_2-dpph** (lower, λ_{em} = 548 nm) under degassed condition. **c**: Schematic image of lanthanide emission in the **Eu_2-dpph** and **Tb_2-dpph** crystals. Red balls represent Eu^{3+} or Tb^{3+}.

Mixed lanthanide crystals, $[Eu_xLu_{2-x}(tmh)_6dpph]$ (**Eu_xLu_{2-x}-dpph**) and $[Tb_xLu_{2-x}(tmh)_6dpph]$ (**Tb_xLu_{2-x}-dpph**), were prepared by complexation of the dpph ligand with $[Lu(tmh)_3]$ and either $[Eu_2(tmh)_6]$ or $[Tb_2(tmh)_6]$ in methanol. The Eu^{3+} or Tb^{3+} ions were mixed at concentrations of 1, 5, or 10 mol%. Inductively coupled plasma atomic emission spectroscopy (ICP-AES) revealed the molar ratios for **Eu_xLu_{2-x}-dpph** (x = 0.010, 0.028, or 0.084) and **Tb_xLu_{2-x}-dpph** (x = 0.013, 0.060, or 0.140). The powder X-ray diffraction (PXRD) patterns of the lanthanide mixed crystals were similar to that of **Lu_2-dpph** (**Figure S20**), suggesting similar crystal structures.

The emission spectral shapes of **Eu_xLu_{2-x}-dpph** and **Tb_xLu_{2-x}-dpph** (**Figure 4a** and **S21**) are almost identical to those of **Eu_2-dpph** and **Tb_2-dpph**, respectively. Their photophysical properties are summarized in **Table 1**. The emission photographs of **$Eu_{0.010}Lu_{1.990}$-dpph** and **$Tb_{0.013}Lu_{1.987}$-dpph** are depicted in **Figure 4b**. **Eu_xLu_{2-x}-dpph** exhibits a significantly extended emission decay time range compared with that of **Eu_2-dpph** (**Figure 4c** and **S22**), which increases with decreasing Eu^{3+} molar ratios. The decay curves are fitted to triple-exponential functions (**Table S3**). In contrast to the single-exponential decay observed in **Eu_2-dpph** and **Tb_2-dpph**, the multi-exponential decay behavior in **Eu_xLu_{2-x}-dpph** and **Tb_xLu_{2-x}-dpph** suggests the presence of intermolecular triplet exciton migration (**Figure 4d**). The average emission lifetime (τ_{avg}) for **$Eu_{0.010}Lu_{1.990}$-dpph, $Eu_{0.028}Lu_{1.972}$-dpph**, **$Eu_{0.084}Lu_{1.916}$-dpph** is estimated to be 7.42, 3.54, and 1.22 ms, respectively. **Tb_xLu_{2-x}-dpph** also shows similar photophysical properties, with the τ_{avg} values for **$Tb_{0.013}Lu_{1.987}$-dpph**, **$Tb_{0.060}Lu_{1.940}$-dpph**, and **$Tb_{0.140}Lu_{1.860}$-dpph** being 7.80, 2.14, and 1.31 ms, respectively. Thus, we successfully demonstrated a method for extending the emission lifetime *via* triplet exciton migration in an aggregation system composed of lanthanide complexes.

Table 1. Photophysical properties of lanthanide molecular crystals. τ_{avg}: average emission lifetime; Φ_{tot}: total emission quantum yield based on ligand excitation; I_B: brightness.

Compounds	τ_{avg}[a] / ms	Φ_{tot}[b] / %	I_B [d] / M^{-1} cm^{-1}
Eu_2-dpph	0.55	9.8±0.7	56.4
$Eu_{0.084}Lu_{1.916}$-dpph	1.22	23.5±0.1	135
$Eu_{0.028}Lu_{1.972}$-dpph	3.54	19.9±0.9	114
$Eu_{0.010}Lu_{1.990}$-dpph	7.42	14.0±1.3	80.5
$Eu_{0.005}Lu_{1.995}$-dcph	148	3.0±2.0	26.2
Tb_2-dpph	0.83[c]	67.9±0.8	390
$Tb_{0.140}Lu_{1.860}$-dpph	1.31	38.2±0.7	220
$Tb_{0.060}Lu_{1.940}$-dpph	2.14	34.7±0.8	200
$Tb_{0.013}Lu_{1.987}$-dpph	7.80	18.5±0.8	106
$Tb_{0.011}Lu_{1.989}$-dcph	152	28.7±1.3	250

[a] λ_{ex} = 356 nm, λ_{em} = 612 nm (for **Eu_xLu_{2-x}-dpph**), 608 nm (for **$Eu_{0.005}Lu_{1.995}$-dpph**) or 548 nm (for **Tb_xLu_{2-x}-dpph**, **$Tb_{0.011}Lu_{1.989}$-dcph**), under degassed condition, crystalline state. [b] λ_{ex} = 356 nm, N_2 atmosphere, crystalline state. [c] Ref. [25]. [d] λ_{ex} = 356 nm.

The optical codes were also tunable *via* ligand modification. The preparation and identification of **Lu_2-dcph**, **$Eu_{0.005}Lu_{1.995}$-dcph** and **$Tb_{0.011}Lu_{1.989}$-dcph** were performed using the same procedures as those for **Lu_2-dpph**, **Eu_xLu_{2-x}-dpph** and **Tb_xLu_{2-x}-dpph**, respectively. The PXRD patterns of **$Eu_{0.005}Lu_{1.995}$-dcph** and **$Tb_{0.011}Lu_{1.989}$-dcph** were similar to those of **Lu_2-dcph** (**Figure S23**), suggesting similar crystal structures. The emission spectrum of **$Eu_{0.005}Lu_{1.995}$-dcph** (**Figure S24**) depicts emission bands at approximately 578, 594, 608, 655, and 701 nm were observed, which are assigned to the $^5D_0 \rightarrow {}^7F_J$ (J = 0, 1, 2, 3, and 4, respectively) transitions of Eu^{3+}. For **$Tb_{0.011}Lu_{1.989}$-dcph**, emission bands at approximately 489, 548, 581, 616, and 679 nm were observed. These emission bands are attributed to the $^5D_4 \rightarrow {}^7F_J$ (J = 6, 5, 4, 3, and 2, respectively) transitions of Tb^{3+}. The emission lifetimes of **Lu_2-dcph**, **$Eu_{0.005}Lu_{1.995}$-dcph**, **$Tb_{0.011}Lu_{1.989}$-dcph** are significantly extended (τ_{avg} = 246, 148, and 152 ms, respectively; **Table1**, **Figure 4b,** and **Supplementary Note 3**).

To reveal the origin of the significantly extended emission lifetime, single-crystal XRD analysis for **Lu_2-dcph** was conducted (**Figure S26**, crystallographic parameters are shown in **Table S4**). From the X-ray crystal structure, one phenanthrene unit in the Lu^{3+} complex is surrounded by two adjacent phenanthrene units at a distance of 1.14 nm (**Figure S27**), which is larger than those in **Lu_2-dpph** (1.02 and 1.05 nm). According to the Dexter-type TTET model, the TTET rate exhibits exponential decrease with increasing donor-acceptor distance.[31] Previous studies indicate that even a 0.1 nm change in the long-range region (> 1.0 nm) can lead to an effective change in the TTET rate.[32-34] The increased distance of approximately 0.1 nm can contribute to the extended lanthanide emission lifetime. Moreover, deactivation rate from the triplet state is also a factor contributing to extended emission lifetime. The total emission quantum yield (Φ_{tot}) for Tb^{3+} emission of **Tb_2-dcph** (Φ_{tot} = 63.0%, **Supplementary Note 4**) is marginally lower than that of the **Tb_2-dpph** (Φ_{tot} = 67.9%, **Table 1**). Conversely, the Tb^{3+} emission quantum yield for **$Tb_{0.011}Lu_{1.989}$-dcph** (Φ_{tot} = 28.7%) is higher than that of **$Tb_{0.013}Lu_{1.987}$-dpph** (Φ_{tot} = 18.5%). These results indicate that more efficient intermolecular TTET occurred in the **$Tb_{0.011}Lu_{1.989}$-dcph** crystal, which is considered to be a smaller deactivation rate from the dcph triplet state in the complex unit. Thus, these combined effects of increased intermolecular distance and long-lived triplet state synergistically contribute to the significantly extended lanthanide emission lifetime in the present triplet exciton migration system.

The space-fill drawing models for **Lu_2-dpph** and **Lu_2-dcph** are shown in **Figure S30** to discuss the origin of the long-lived T_1 state in **Lu_2-dcph**. The space-fill drawing model for **Lu_2-dcph** indicates that the central phenanthrene ring is more sterically protected by the surrounding bulky tmh ligands than that in **Lu_2-dpph**. This enhanced steric protection is considered to suppress the torsional distortion of the phenanthrene unit, thereby suppressing access to conical intersections.[35]

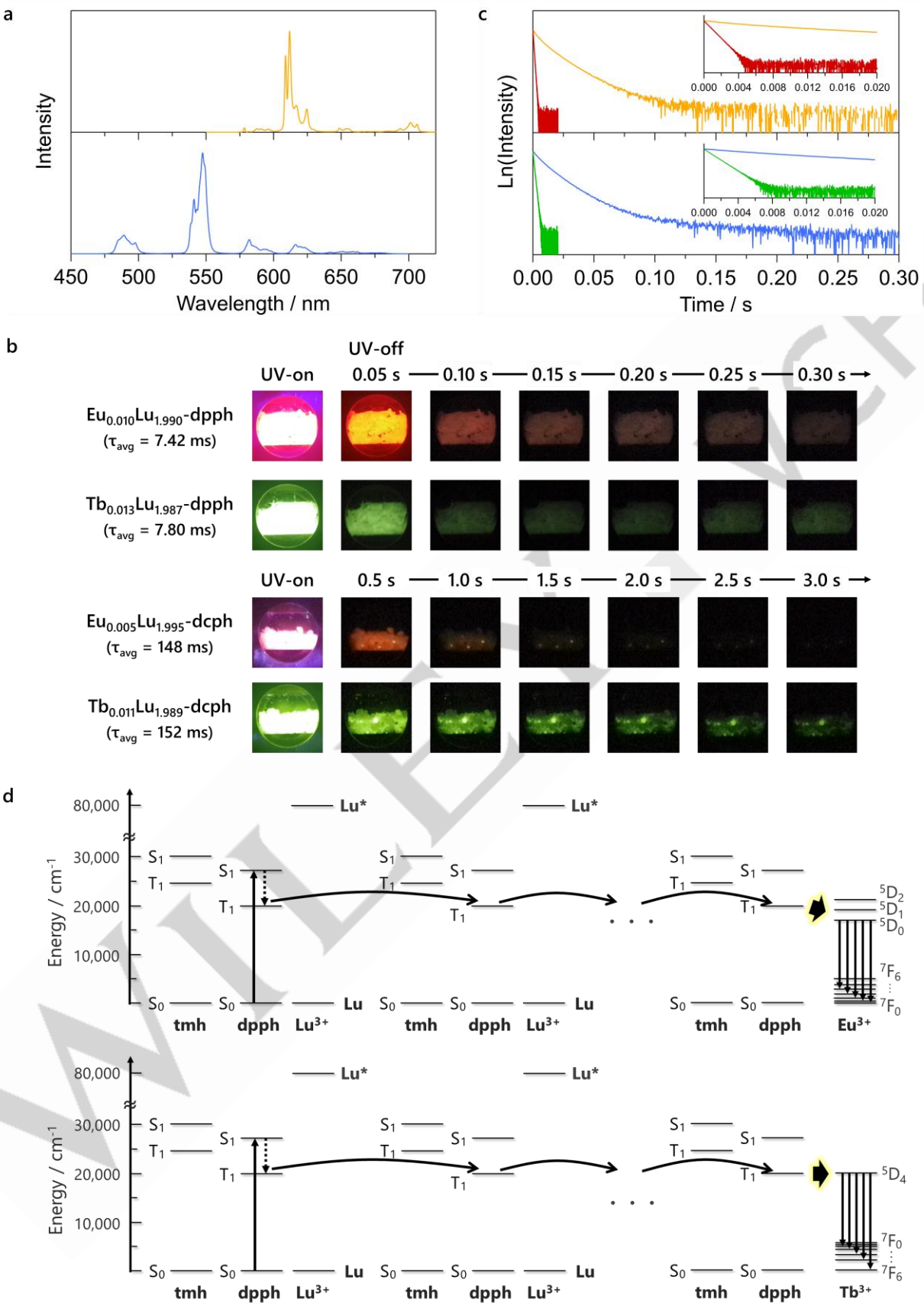

Figure 4. a: Emission spectra (λ_{ex} = 356 nm, degassed condition, crystalline state, 293 K) of **$Eu_{0.010}Lu_{1.990}$-dpph** (orange line) and **$Tb_{0.013}Lu_{1.987}$-dpph** (blue line). **b**: Emission photographs (λ_{ex} = 375 nm, degassed condition, crystalline state, 293 K) of **$Eu_{0.010}Lu_{1.990}$-dpph**, **$Tb_{0.013}Lu_{1.987}$-dpph**, **$Eu_{0.005}Lu_{1.995}$-dcph**, and **$Tb_{0.011}Lu_{1.989}$-dcph**. **c**: Emission decay curves (λ_{ex} = 356 nm, degassed condition, crystalline state, 293 K) of **$Eu_{0.010}Lu_{1.990}$-dpph** (upper, orange line, λ_{em} = 612 nm), **Eu_2-dpph** (upper, red line), **$Tb_{0.013}Lu_{1.987}$-dpph** (lower, blue line, λ_{em} = 548 nm), and **Tb_2-dpph** (lower, green line). **d**: Energy diagrams of **$Eu_{0.010}Lu_{1.990}$-dpph** and **$Tb_{0.013}Lu_{1.987}$-dpph**.

The emission intensity is also a critical factor for optical encoders. For **Tb_xLu_{2-x}-dpph**, the total emission quantum yield depends on the molar ratio of Tb^{3+} (**Table 1**, Φ_{tot} = 67.9% (x = 2), 38.2% (x = 0.140), 34.7% (x = 0.060), 18.5% (x = 0.013)). The brightness values (I_B) are estimated using the following equation:[36]

$$I_B = \varepsilon \times \phi_{tot}$$

where ε is the absorption coefficient (**Figure S31**). The I_B values are estimated to be 390 (x = 2), 220 (x = 0.140), 200 (x = 0.060), and 106 (x = 0.013) M^{-1} cm^{-1}, respectively (**Table 1**). Despite the dilution of the Tb^{3+} ion, the brightness of **Tb_xLu_{2-x}-dpph** is much higher than that expected from the dilution degree, indicating effective photosensitization *via* intermolecular energy transfer between the lanthanide complexes.

The total emission quantum yields for **Eu_xLu_{2-x}-dpph** change characteristically with decreasing Eu^{3+} molar ratios (Φ_{tot} = 9.8% (x = 2), 23.5% (x = 0.084), 19.9% (x = 0.028), and 14.0% (x = 0.010)). The photophysical analyses reveal that the low Φ_{tot} for **Eu_2-dpph** (9.8%) is due to its low photosensitization efficiency (η_{sens} = 17.8%, **Supplementary Note 2**). According to previous reports, the low photosensitization efficiency for **Eu_2-dpph** is attributed to the formation of ligand-to-metal charge transfer (LMCT) states in the lower-energy region than that for the ligand excited singlet state.[37-40] A relatively high HOMO level of the tmh ligands (–5.12 eV[25]) promotes the formation of LMCT states in the visible region, which can induce energy transfer quenching from the dpph singlet state. The formation of dpph singlet states in the Eu^{3+} complex leads to energy transfer quenching to a LMCT state, resulting in inefficient photosensitized Eu^{3+} emission. The mixed crystals (**Eu_xLu_{2-x}-dpph**) suppress the formation of the dpph singlet state in the Eu^{3+} complex units by intermolecular photosensitization *via* TTET, resulting in higher brightness values (I_B = 135 (x = 0.084), 114 (x = 0.028), and 80.5 (x = 0.010) M^{-1} cm^{-1}) than that of **Eu_2-dpph** (I_B = 56.4 M^{-1} cm^{-1}).

The total emission quantum yields for **$Eu_{0.005}Lu_{1.995}$-dcph** and **$Tb_{0.011}Lu_{1.989}$-dcph** were estimated to be 3.0% and 28.7%, respectively (**Table 1**). Their I_B values were calculated as 26.2 and 250 M^{-1} cm^{-1} for **$Eu_{0.005}Lu_{1.995}$-dcph** and **$Tb_{0.011}Lu_{1.989}$-dcph**, respectively. Although the Eu^{3+} and Tb^{3+} concentrations in the mixed lanthanide crystals are significantly lower than those in pure lanthanide crystals ([$Eu_2(tmh)_6$dcph]: I_B = 45.3 M^{-1} cm^{-1} and [$Tb_2(tmh)_6$dcph]: I_B = 549 M^{-1} cm^{-1}, **Supplementary Note 4**), the I_B values of **$Eu_{0.005}Lu_{1.995}$-dcph** and **$Tb_{0.011}Lu_{1.989}$-dcph** are much higher than those expected based on the dilution degree from [$Eu_2(tmh)_6$dcph] and [$Tb_2(tmh)_6$dcph], which indicates effective photosensitization *via* TTET.

In this study, Eu^{3+}-Lu^{3+} and Tb^{3+}-Lu^{3+} mixed lanthanide crystals were prepared to demonstrate a method for controlling the emission lifetime using an aggregation system. The emission lifetime was effectively extended by slow intermolecular triplet exciton migration in the crystals. The emission lifetime (Eu^{3+}: 0.55–148 ms, Tb^{3+}: 0.83–152 ms) can be markedly tuned by varying the molar ratio of Eu^{3+} (or Tb^{3+}) or modifying the ligands. The present mechanism is expected to allow greater extension of emission lifetime (> 200 ms) using organic ligands with longer-lived triplet excitons. Long-lived triplet exciton migration also provides high brightness for an effective optical encoder. This method significantly expands the optical encoding capacity of lanthanide complexes. Water-soluble nanoparticles and amorphous films in aggregated states will be key designs for the development of applications in multiplexed bioimaging and anti-counterfeiting, respectively. The proposed dynamic triplet exciton system can significantly impact on the fields of bio-chemistry and analytical chemistry.

Supporting Information

The authors have cited additional references within the Supporting Information.[41-44]

Acknowledgements

This work was partially supported by a Grants-in-Aid for Scientific Research (grant numbers JP24K21774, JP23H04863, and JP20H02748) and by a JSPS Research Fellow (JP24KJ0312). This work was also supported by the Adaptable and Seamless Technology Transfer Program through Target-driven R&D (A-STEP) from the Japan Science and Technology Agency (JST), Japan (Grant Number JPMJTR23T5), and the Institute for Chemical Reaction Design and Discovery (ICReDD), established by the World Premier International Research Center Initiative (WPI) of MEXT, Japan.

Keywords: lanthanide • optical encoding • molecular crystals

Author Contributions

Y.K. designed the research. T.Nakai and K.S. performed syntheses and measurements. T.Nakanishi and Y.H. supported the optical measurements. T.Nakai and Y.K. wrote the paper. All authors discuss and review the paper.

References

[1] H. H. Gorris, O. S. Wolfbeis, "Photon-Upconverting Nanoparticles for Optical Encoding and Multiplexing of Cells, Biomolecules, and Microspheres" *Angew. Chem. Int. Ed.* **2013**, 52, 3584–3600.

[2] Y. Fan, S. Wang, F. Zhang, "Optical Multiplexed Bioassays for Improved Biomedical Diagnostics" *Angew. Chem. Int. Ed.* **2019**, 58, 13208–13219.

[3] G. Lin, M. A. B. Baker, M. Hong, D. Jin, "The Quest for Optical Multiplexing in Bio-discoveries" *Chem* **2018**, 4, 997–1021.

[4] J. Xu, J. Zhou, Y. Chen, P. Yang, J. Lin, "Lanthanide-Activated Nanoconstructs for Optical Multiplexing" *Coord. Chem. Rev.* **2020**, 415, 213328.

[5] Y. Fan, P. Wang, Y. Lu, R. Wang, L. Zhou, X. Zheng, X. Li, J. A. Piper, F. Zhang, "Lifetime-Engineered NIR-II Nanoparticles Unlock Multiplexed in Vivo Imaging" *Nat. Nanotechnol.* **2018**, 13, 941–946.

[6] T. Wang, S. Wang, Z. Liu, Z. He, P. Yu, M. Zhao, H. Zhang, L. Lu, Z. Wang, Z. Wang, W. Zhang, Y. Fan, C. X. Sun, D. Zhao, W. Liu, J.-C. G. Bünzli, F. Zhang, "A Hybrid Erbium(III)–Bacteriochlorin Near-Infrared Probe for Multiplexed Biomedical Imaging" *Nat. Mater.* **2021**, 20, 1571–1578.

[7] H. Li, M. Tan, X. Wang, F. Li, Y. Zhang, L. Zhao, C. Yang, G. Chen, "Temporal Multiplexed in Vivo Upconversion Imaging" *J. Am. Chem. Soc.* **2020**, 142, 2023–2030.

[8] X. Qiu, J. Xu, M. C. D. Santos, N. Hildebrandt, "Multiplexed Biosensing and Bioimaging Using Lanthanide-Based Time-Gated Förster Resonance Energy Transfer" *Acc. Chem. Res.* **2022**, 55, 551–564.

[9] W. Yao, Q. Tian, W. Wu, "Tunable Emissions of Upconversion Fluorescence for Security Applications" *Adv. Opt. Mater.* **2019**, 7, 1801171.

[10] Y. Lu, J. Zhao, R. Zhang, Y. Liu, D. Liu, E. M. Goldys, X. Yang, P. Xi, A. Sunna, J. Lu, Y. Shi, R. C. Leif, Y. Huo, J. Shen, J. A. Piper, J. P. Robinson, D. Jin, "Tunable Lifetime Multiplexing using Luminescent Nanocrystals" *Nat. Photon.* **2014**, 8, 33–37.

[11] M. Tan, F. Li, X. Wang, R. Fan, G. Chen, "Temporal Multilevel Luminescence Anticounterfeiting through Scattering Media" *ACS Nano* **2020**, 14, 6532–6538.

[12] B. Zhou, B. Shi, D. Jin, X. Liu, "Controlling Upconversion Nanocrystals for Emerging Applications" *Nat. Nanotechnol.* **2015**, 10, 924–936.

[13] J. I. Deneff, L. E. S. Rohwer, K. S. Butler, B. Kaehr, D. J. Vogel, T. S. Luk, R. A. Reyes, A. A. Cruz-Cabrera, J. E. Martin, D. F. S. Gallis, "Orthogonal Luminescence Lifetime Encoding by Intermetallic Energy Transfer in Heterometallic Rare-Earth MOFs" *Nat. Commun.* **2023**, 14, 981.

[14] Y. Qu, W. Zhou, Z. Zhu, F. Ma, R. Zhou, F. Su, L. Zheng, L. Ma, H. Liang, "Host Differential Sensitization toward Color/Lifetime-Tuned Lanthanide Coordination Polymers for Optical Multiplexing" *Angew. Chem. Int. Ed.* **2020**, 59, 23810–23816.

[15] J. Jia, P. Ren, H. Hu, N. Sayyadi, F. Pavin, X. Zheng, B. Shi, J. A. Piper, B. Song, K. Vickery, and Y. Lu, "Lifetime Multiplexing with Lanthanide Complexes for Luminescence in Situ Hybridisation" *Analysis & Sensing* **2021**, 2, e202100057.

[16] Y. Lu, J. Lu, J. Zhao, J. Cusido, F. M. Raymo, J. Yuan, S. Yang, R. C. Leif, Y. Huo, J. A. Piper, J. P. Robinson, E. M. Goldys, D. Jin, "On-the-Fly Decoding Luminescence Lifetimes in the Microsecond Region for Lanthanide-Encoded Suspension Arrays" *Nat. Commun.* **2014**, 5, 3741.

[17] D. Kovacs, X. Lu, L. S. Mészáros, M. Ott, J. Andres, K. E. Borbas, "Photophysics of Coumarin and Carbostyril-Sensitized Luminescent Lanthanide Complexes: Implications for Complex Design in Multiplex Detection" *J. Am. Chem. Soc.* **2017**, 139, 5756–5767.

[18] V. Placide, A. T. Bui, A. Grichine, A. Duperray, D. Pitrat, C. Andraud, O. Maury, "Two-Photon Multiplexing Bio-Imaging Using a Combination of Eu- and Tb-Bioprobes" *Dalton Trans.* **2015**, 44, 4918–4924.

[19] Z. Liao, M. Tropiano, S. Faulkner, T. Vosch, T. J. Sørensen, "Time-Resolved Confocal Microscopy Using Lanthanide Centred Near-IR Emission" *RSC Adv.* **2015**, 5, 70282–70286.

[20] E. Pershagen, K. E. Borbas, "Multiplex Detection of Enzymatic Activity with Responsive Lanthanide-Based Luminescent Probes" *Angew. Chem. Int. Ed.* **2015**, 54, 1787–1790.

[21] M. Sy, A. Nonat, N. Hildebrandt, L. J. Charbonniére, "Lanthanide-based Luminescence Biolabelling" *Chem. Commun.* **2016**, 52, 5080–5095.

[22] K. Binnemans, "Lanthanide-Based Luminescent Hybrid Materials" *Chem. Rev.* **2009**, 109, 4283–4374.

[23] J.-C. G. Bünzli, "On the Design of Highly Luminescent Lanthanide Complexes" *Coord. Chem. Rev.* **2015**, 293, 19–47.

[24] D. Parker, J. D. Fradgley, K.-L. Wong, "The Design of Responsive Luminescent Lanthanide Probes and Sensors" *Chem. Soc. Rev.* **2021**, 50, 8193–8213.

[25] Y. Kitagawa, K. Shima, T. Nakai, M. Kumagai, S. Omagari, P. P. Ferreira da Rosa, S. Shoji, K. Fushimi, Yasuchika Hasegawa, "Thermally-Assisted Photosensitized Emission in a Trivalent Terbium Complex" *Commun. Chem.* **2023**, 6, 122.

[26] P. Dorenbos, "The 5d Level Positions of the Trivalent Lanthanides in Inorganic Compounds" *J. Lumin.* **2000**, 91, 155–176.

[27] A. Masuya-Suzuki, S. Goto, R. Nakamura, R. Karashimada, Y. Kubota, R. Tsunashima, N. Iki, "Emergence of the Super Antenna Effect in Mixed Crystals of Ytterbium and Lutetium Complexes Showing Near-Infrared Luminescence" *RSC Adv.* **2022**,12, 30598–30604.

[28] S. Miyazaki, K. Miyata, H. Sakamoto, F. Suzue, Y. Kitagawa, Y. Hasegawa, K. Onda, "Dual Energy Transfer Pathways from an Antenna Ligand to Lanthanide Ion in Trivalent Europium Complexes with Phosphine-Oxide Bridges" *J. Phys. Chem. A* **2020**, 124, 6601–6606.

[29] S. I. Klink, L. Grave, D. N. Reinhoudt, F. C. J. van Veggel, M. H. V. Werts, F. A. J. Geurts, J. W. Hofstraat, "A Systematic Study of the Photophysical Processes in Polydentate Triphenylene-Functionalized Eu^{3+}, Tb^{3+}, Nd^{3+}, Yb^{3+}, and Er^{3+} Complexes" *J. Phys. Chem. A* **2000**, 104, 5457–5468.

[30] M. W. Mara, D. S. Tatum, A.-M. March, G. Doumy, E. G. Moore, K. N. Raymond, "Energy Transfer from Antenna Ligand to Europium(III) Followed Using Ultrafast Optical and X-ray Spectroscopy" *J. Am. Chem. Soc.* **2019**, 141, 11071–11081.

[31] D. L. Dexter, "A Theory of Sensitized Luminescence in Solids" *J. Chem. Phys.* **1953**, 21, 836–850.

[32] S. Häcker, T. J. B. Zähringer, H.-A. Wagenknecht, C. Kerzig, "Direct Observation of Triplet–Triplet Energy Transfer in DNA between Energy Donor and Acceptor C-Nucleotides" *JACS Au* **2025**, 5, 2770–2778.

[33] B. Albinsson, J. Martensson, "Excitation Energy Transfer in Donor–Bridge–Acceptor Systems" *Phys. Chem. Chem. Phys.* **2010**, 12, 7338–7351.

[34] O. S. Wegner, "Photoinduced Electron and Energy Transfer in Phenylene Oligomers" *Chem. Soc. Rev.* **2011**, 40, 3538–3550.

[35] Y. Harabuchi, T. Taketsugu, S. Maeda, "Exploration of Minimum Energy Conical Intersection Structures of Small Polycyclic Aromatic Hydrocarbons: Toward an Understanding of the Size Dependence of Fluorescence Quantum Yields" *Phys. Chem. Chem. Phys.* **2015**, 17, 22561–22565.

[36] K.-L. Wong, J.-C. G. Bünzli, P. A. Tanner, "Quantum Yield and Brightness" *J. Lumin.* **2020**, 224, 117256.

[37] P. P. Ferreira da Rosa, S. Miyazaki, H. Sakamoto, Y. Kitagawa, K. Miyata, T. Akama, M. Kobayashi, K. Fushimi, K. Onda, T. Taketsugu, Y. Hasegawa, "Coordination Geometrical Effect on Ligand-to-Metal Charge Transfer-Dependent Energy Transfer Processes of Luminescent Eu(III) Complexes" *J. Phys. Chem. A* **2021**, 125, 209–217.

[38] Y. Kitagawa, P. P. Ferreira da Rosa, Y. Hasegawa, "Charge-Transfer Excited States of π- and 4f-Orbitals for Development of Luminescent Eu(iii) Complexes" *Dalton Trans.*, **2021**, 50, 14978-14984.

[39] G. D. R. Napier, R. J. D. Neilson, T. M. Shepherd, "Charge-Transfer Excited State in Tris(acetylacetonato) Europium(III)" *Chem. Phys. Lett.*, **1975**, 31, 328–330.

[40] Y. C. Miranda, L. L. A. L. Pereira, J. H. P. Barbosa, H. F. Brito, M. C. F. C. Felinto, O. L. Malta, W. M. Faustino and E. E. S. Teotonio, "The Role of the Ligand-to-Metal Charge-Transfer State in the Dipivaloylmethanate-Lanthanide Intramolecular Energy Transfer Process" *Eur. J. Inorg. Chem.*, **2015**, 18, 3019–3027.

[41] G. M. Sheldrick, "A short history of SHELX" *Acta Crystallogr. Sect. A Found. Crystallogr.* **2008**, 64, 112–122.

[42] O. V. Dolomanov, L. J. Bourhis, R. J. Gildea, J. A. K. Howard, H. Puschmann, "OLEX2: a Complete Structure Solution, Refinement and Analysis Program" *J. Appl. Crystallogr.* **2009**, 42, 339–341.

[43] M. H. V. Werts, R. T. F. Jukes, J. W. Verhoeven, "The Emission Spectrum and the Radiative Lifetime of Eu^{3+} in Luminescent Lanthanide Complexes" *Phys. Chem. Chem. Phys.* **2002**, 4, 1542–1548.

[44] M. MacDonald, J. Bates, J. Ziller, F. Furche, W. Evans, "Completing the Series of +2 Ions for the Lanthanide Elements: Synthesis of Molecular Complexes of Pr^{2+}, Gd^{2+}, Tb^{2+}, and Lu^{2+}" *J. Am. Chem. Soc.* **2013**, 135, 9857–9868.

Entry for the Table of Contents

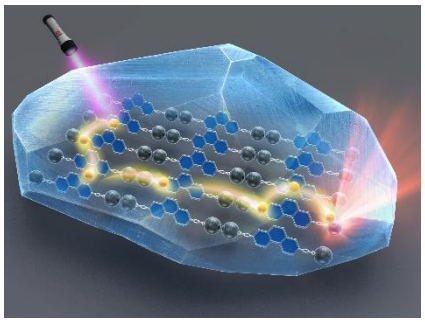

The Eu^{3+}-(or Tb^{3+}-)-incorporated Lu^{3+} molecular crystals were prepared for the demonstration of emission lifetime tuning method using slow triplet exciton migration. The lanthanide emission lifetimes were drastically extended (τ_{max} = 152 ms) by controlling the molar ratios of Eu^{3+} (or Tb^{3+}) and modifying the ligand structures.